Landslide hazard evaluation and zonation in Dilbe Town and its surrounding areas, North-western Central Ethiopia – A GIS based grid overlay statistical approach

Sendu Demessie[1] and Tarun Kumar Raghuvanshi[2]*
[1]Department of Geology, Woldia University, PO Box 400, Woldia, Ethiopia
[2]School of Earth Sciences, College of Natural Sciences, PO Box 1176, Addis Ababa University, Addis Ababa, Ethiopia
*Email: tkraghuvanshi@gmail.com

(Received: Apr 04, 2019; in final form: June 18, 2019)

Abstract: The present study was carried out in Dilbe town and its surrounding areas, North-western Central Ethiopian, located about 576 km from Addis Ababa city. The main objective of the present study was to carry out landslide evaluation and Zonation of the study area for which an integrated GIS based Grid overlay statistical approach was followed. For landslide hazard zonation (LHZ) six causative factors; slope-material, slope, aspect, elevation, land use/land cover and groundwater surface traces were considered. These causative factors were derived from topographical sheets, secondary maps, digital elevation model and through field investigation. The quantitative relationship between these causative factors and the past landslides in the area was made through overlay analysis and the Landslide susceptibility index (LSI) was computed. Further, geo-processing was done by overlaying a polygon grid (10x10 m) over each factor map in GIS environment. This forms the basis to evaluate LHZ map of the study area. The results showed that 11.55% of the study area falls into 'very high hazard', 19.84% area falls into 'high hazard', 14.36% area fall into 'medium hazard', 38.25% area falls into 'low hazard' and remaining 16% of the area falls into 'very low hazard'. Further, validation results showed that 74% of the past landslides fall within 'very high hazard' and 'high hazard' zones of the prepared LHZ map. The prepared LHZ map has reasonably validated with the past landslide data. Thus, various landslide hazard zones delineated can safely be applied for future developmental planning in the present study area.

Keywords: Landslides, Landslide hazard evaluation, Landslide susceptibility index, Landslide hazard zonation

1. Introduction

Landslides are well known devastating natural hazard in mountainous terrain. The landslides result into wide spread damage to the infrastructure, land degradation and significant loss to the human life and injury throughout the world (Varnes, 1996; Parise and Jibson, 2000; Dai et al., 2002; Sarkar and Kanungo, 2004; Crozier and Glade, 2005; Kanungo et al., 2006; Pan et al., 2008; Marraqu and Jakka, 2014; Raghuvanshi et al., 2014a; Girma et al., 2015; Raghuvanshi et al., 2015). Several internal and external factors, in combination, result into landslide. The primary internal factors are related to geo-morphology, geology and hydrology (Anbalagan, 1992; Ayalew et al., 2004; Wang and Niu, 2009; Hamza and Raghuvanshi, 2017) whereas main external factors are rainfall (Collison et al., 2000; Dai and Lee, 2001; Dahal et al., 2006; Raghuvanshi et al., 2014a), seismicity (Parise and Jibson, 2000; Keefer, 2000; Bommer and Rodrı´guez, 2002; Raghuvanshi et al., 2014a) and manmade activities (Gorsevski et al., 2006; Raghuvanshi et al., 2014a). These factors are responsible for slope failure either by reducing the shear strength of the slope material or these factors may increase the shear forces (Sarkar and Kanungo, 2004).

Landslide hazard evaluation and zonation involves delineation of future hazardous zones based on analysis of governing parameters (Arnous, 2011) and to classify land into different zones of potential or actual landslide hazard (Varnes, 1984; Anbalagan, 1992; Raghuvanshi et al., 2014a). In order to carryout landslide hazard evaluation, prediction and zonation, several techniques are proposed by different researchers which can broadly be classified into expert evaluation (Anbalagan, 1992; Raghuvanshi et al., 2014b), statistical methods (Carrara et al., 1992; WestenVan et al., 1997; Dai and Lee, 2001) and the deterministic approach (Fall et al., 2006; Raghuvanshi et al., 2015). Each of these techniques has their own merit and demerits over others (Leroi, 1997; Guzzetti et al., 1999; Casagli et al., 2004; Kanungo et al., 2006; Fall et al., 2006; Raghuvanshi et al., 2014a; 2014b). The selection of a technique for landslide hazard zonation primarily depends on factors, namely; area to be covered for hazard zonation, scale at which zonation has to be done, geological and geo-morphological factors to be considered, method by which parameter data has to be acquired and skill set or capability of an evaluator (Carrara, 1992; Ermias et al., 2017).

In Ethiopia, landslide is a common geo-environmental hazard in the highlands (Ayalew and Yamagishi, 2004; Ayenew and Barberie, 2005; Abebe et al., 2010; Raghuvanshi, 2014a; 2014b). The present study area, Dilbe town and its surrounding area, which is located in the north western central Ethiopian highland, is a rugged mountainous terrain. The area is well known for its devastating landslides which has caused considerable damage to the roads, houses and the agricultural land in the area. Thus, there was a necessity to evaluate and carry out landslide hazard zonation in the area, so that concerned authorities and local people may be made aware about the hazardous zones in the area. Such information may be helpful for the safe land use planning and development in the area. Besides, this may also help to mitigate the problems related to landslides in the study area. The main objective of the present study was to evaluate the factors influencing the landslide hazard and to produce the landslide Hazard Zonation (LHZ) map of the study area.

2. The Study area

The present study area is located in the North-western central Ethiopia, North Wello Zone in Gubalafto District (Figure 1). The total study area is about 50 km^2. The study area is bounded by UTM co-ordinates 1318000m to 1326500m N and 543200m to 552800mE. The study area is about 576 km from Addis Ababa, the capital city of Ethiopia, on way to Woldiya Town. The elevation in general ranges from 2243m to 3591m a.s.l. The study area has rugged topography and is characterized by sharp valleys, hills and ridges. The climate of the area is characterized as temperate (Gemechu, 1997). The long term average mean annual rainfall in the study area is 661.5 mm (1995 to 2016) and the maximum monthly average precipitation recorded was 401.7 mm in the month of August in 2010. The maximum and minimum temperature in the area is 24.3^o C and 1.2^o C, respectively. The drainage in the study area is characterized as dendritic to sub parallel and all major and minor streams drain into Gembora River.

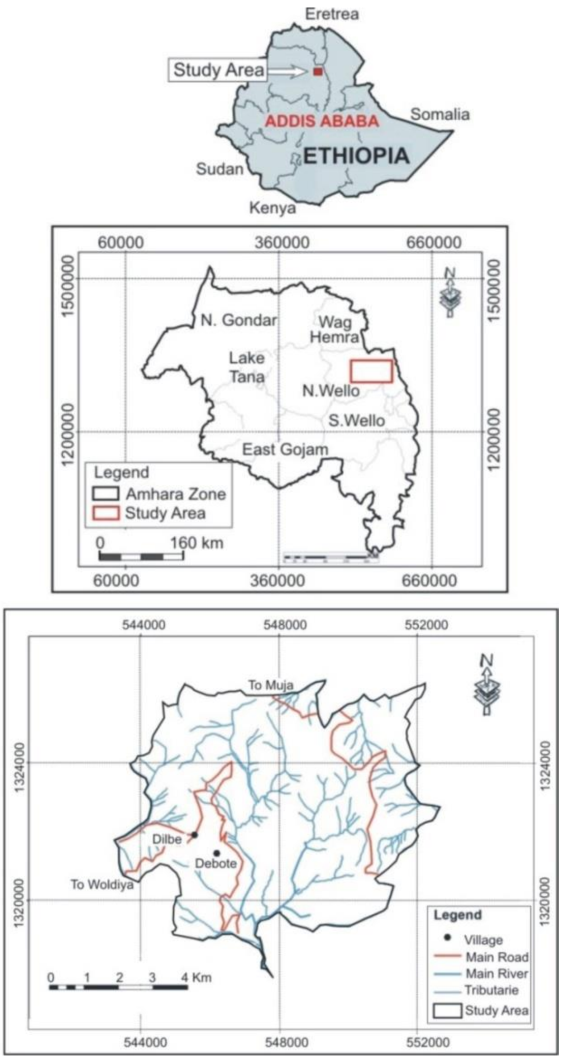

Figure 1: Location map of the study area

3. Geology

The present study area is located in the South-western block of the Afar Depression, where the Main Ethiopian Rift (MER) gradually funnels towards the Afar Depression. Ashangi basalts are the earliest fissural volcanic rocks exposed in the area (Tefera et al., 1996) which belongs to Eocene-Oligocene period. The Ashangi basalts are followed by Dessie basalt and Tarmaber Megezez Formations, belonging to Oligo-Miocene period (Demissie et al., 2010) (Figure 2). Ashangi basalt Formation is exposed mainly over the steep slopes, low lying flat plains, stream beds and on the gentle slopes. These are overlain un-conformably on the Dessie basalt formation. Ashangi basalts are highly weathered, jointed and fractured and are oriented in different directions (Demissie et al., 2010). Aphanitic basalts with columnar jointing are commonly exposed in the study area which belongs to Ashangi basalt Formation. These rocks are black, dark gray and greenish gray in color with aphanatic to coarse grained in texture. Dessie basalt Formation is mainly exposed in the western plateau area and comprises aphanatic, porphyritic, massive and vesicular basalts (Demissie et al., 2010).The aphanatic basalt belonging to Dessie basalt Formation is dominated by fine microcrystalline matrix with fine plagioclase microlites and porphyritic basalts (Demissie et al., 2010). The Tarmaber Megezez Formation is exposed on the gentle slopes, along the stream beds and along the road sections.

This Formation forms a conformable contact with the Dessie basalt Formation. The rocks belonging to this Formation are characterized by dark gray to black coarse grained vesicular and columnar jointed aphanatic basalts (Demissie et al., 2010).

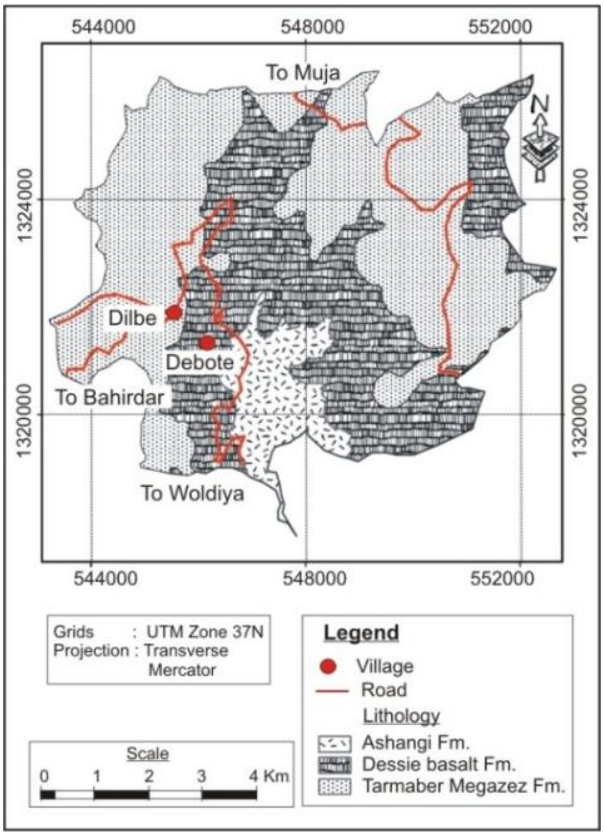

Figure 2: Geology of the study area

4. Methodology

In order to prepare the landslide hazard zonation (LHZ) map of the study area, a GIS based grid overlay statistical approach was followed. This technique was followed as it is based on the principle that "the past and the present are the keys to the future", the future landslides, most likely will occur under similar conditions which has prevailed during the past or the present times (Van Den Eeckhaut et al., 2009). Based on the statistical analysis for the interrelationship of causative factors and the past activities, quantitative estimates can be made for those areas where similar conditions prevailed. Each of the causative factor maps can be overlaid on past landslide map to know the relative contribution for each factor and subclass in inducing landslides in the area. Thus, from this data, respective weights can be developed to be applied to each causative factor subclass and finally a landslide hazard can be deduced for the given area (Dai and Lee, 2001).

For the present study six causative factors; (i) slope material, (ii) slope, (iii) aspect, (iv) elevation, (v) land use/land cover and (vi) groundwater surface traces were considered for the evaluation of LHZ (Ayalew et al., 2004; Girma et al., 2015; Raghuvanshi et al., 2015). Based on the field observations, it was realized that these factors were the significant factors that have resulted into past landslides in the area. It was further assumed that "the past is the key for future" (Varnes, 1984; Carrara et al., 1991). This means that the conditions that were responsible for the past landslides, if reoccur in other areas, again landslides can occur (Dai and Lee, 2001; Raghuvanshi et al., 2015). Thus, in order to understand the relationship of these causative factors with the past landslides, statistical analysis was made between each of the causative factors and the past landslides. For this purpose, individual factor maps were overlaid on the past landslide map in GIS environment and quantitative prediction was made through density analysis between the past landslides and each of the causative factor sub-classes (Dai and Lee, 2001; Lee et al., 2004; Girma et al., 2015; Raghuvanshi et al., 2015; Chimidi et al., 2017; Hamza and Raghuvanshi, 2017). With the help of this statistical density analysis, Landslide Susceptibility Index (LSI) was computed for each parameter sub-class (Raghuvanshi et al., 2015). Further, for grid overlay analysis a polygon grid (10 x 10 m) was overlaid on each parameter theme and geo processing was done to know the presence of each parameter sub-class within each grid cell. Later, respective LSI values for each factor sub-class within each grid cell were assigned. Thus, the sum total of LSI values for six parameters within each grid cell provided Total Landslide Susceptibility Index value (TLSI). These TLSI values were further utilized to define the landslide hazard zonation in the study area.

The present study was carried out in three phases; Pre-field work-desk study, Field investigation and Post field study. During the pre-field-desk study required data from secondary sources was collected. This includes collection of data on meteorology, topographical maps and satellite data. Besides, previous reports, data and maps available for the study area were reviewed. Further, slope facet map, geological and soil cover maps were prepared, later to be utilized during the field work. In addition, digital elevation model (DEM) was obtained at a resolution of 30m from the ASTER data set and factor maps for elevation, slope and aspect were prepared. Also, land use land cover map of the present study area was prepared from the Sentinel-2A data through supervised classification.

The major activities carried out during the field investigation includes inventory mapping for past landslides and verification of the factor maps that were prepared during the pre-field-desk study. The past landslide inventory mapping was carried out by identifying the landslides for its type, dimension, material involved, morphology of failed slope, failure mechanism and the possible triggering factors. The data on landslide inventory was collected through GPS readings along the periphery of the landslide, visual observations on various aspects and through personal interviews with the local residents. Prior to the field work various past landslides in the area were tentatively identified through the Google Earth image and were marked as point data on the facet map. Later during the field work they were further verified and necessary inventory data/ information, as mentioned above were collected.

Besides, factor maps on lithology and soil cover were verified in the field and necessary modifications were made. In order to collect the primary data in the field and to verify factor maps prepared during the pre-field-desk study, slope facet map was used. The facet map was prepared during the pre-field-desk study by delineating major or minor hill ridges and streams on the topographic map by using Arc GIS software (Anbalagan, 1992). Slope facet is basically required to demarcate the area into more or less identical land unit which have nearly similar slope direction and inclination. Therefore, facet provides a means to recognize the land area within which observations can be made. Since, the facets are bounded by streams and ridges therefore they can easily be recognized in the field with the help of topographical map. Thus, the primary purpose of facet is to demarcate the study area into various units which can easily be recognized in the field and within which observations can easily be made for various causative factors.

A total of 54 slope facets were delineated in the study area (Figure 3). In addition, springs present in the study area were located and marked with the help of GPS reading on the elevation map.

The post field study includes processing of data collected during the field investigation stage and to carry out further analysis to prepare landslide hazard zonation map of the study area. The past landslide inventory data, collected as GPS point data along the periphery of the landslides during the field investigation, was converted to polygon data by digitization over the Google-Earth image.

All factor maps and landslide inventory map were brought to the GIS environment for further processing. Besides, individual factor maps were overlaid on past landslide map in GIS environment and quantitative predictions were made through density analysis between the past landslides and each of the causative factor class. Thus, the LSI values for each parameter sub class were computed. Further, overlay analysis was made by overlying grid on each parameter map. Finally, with the help of grid overlay analysis results and the respective LSI values for each factor sub-class, landslide hazard zonation in the study area was worked out. Figure 4 shows the general methodology followed during the present study.

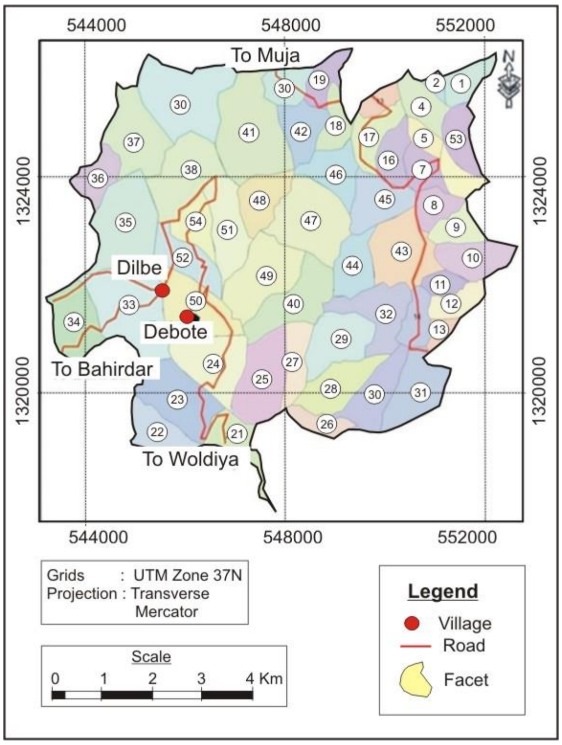

Figure 3: Facet map used for the field data collection

5. Data collection, processing and analysis

For the present study the required data for landslide evaluation and zonation was obtained from the secondary and primary sources. The secondary data that was utilized for the present study includes; topographical maps, geological map, soil cover map, satellite data, digital elevation model (DEM) and the meteorological data (Table 1). The primary data that was used in the present study was mainly obtained through field investigation. This includes verification of factor maps prepared during the pre-field-desk study from secondary data sources and the collection of inventory data and information for the past landslides in the study area.

5.1 Landslide inventory

The landslide inventory data provides useful information in understanding the relative influence of various causative and triggering factors on the slope instability and possible mechanism that has resulted into slope failures. Through landslide inventory data it is possible to understand the conditions that were responsible for the landslides in the area and with this understanding it is possible to know the probable areas where future landslides can occur (Dai et al., 2002; Lan et al., 2004; Raghuvanshi et al., 2015; Chimidi et al., 2017).

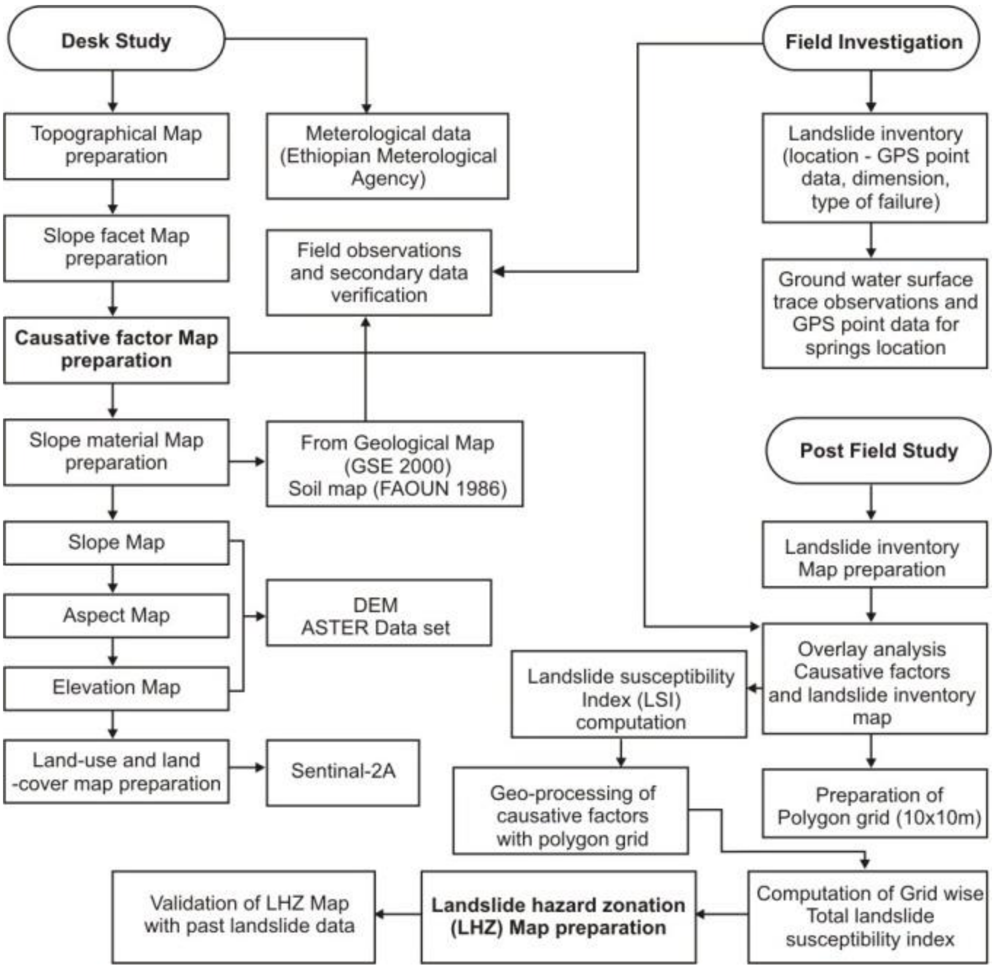

Figure 4: General Methodology followed

Table1: Causative factors respective data source

Causative factors	Data Source
Landslide inventory	Field observations – GPS point data along landslide periphery and by using Google Earth image.
Slope material	Slope material map was prepared from the Geological map of Dessie area prepared by Geological Survey of Ethiopia with a scale of 1:250000 (GSE, 2010), soil map of Ethiopia prepared by Food and Agriculture Organization of United Nations (FAOUN, 1986) and through field investigation and mapping.
Slope Aspect Elevation	DEM data with a resolution of 30 m ASTER elevation data set
Land use land cover	Sentinale-2A and field observation and mapping
Groundwater surface trace	Field observations - GPS point data collected at springs location during field work and delineation of hydrological homogeneous zones over topographical maps.

For the present study landslide inventory data was collected through the field investigation. In order to identify the past landslides in the study area traverse mapping was done and the location of all past landslides was marked over the facet map. Besides, GPS point data was also collected and recorded along the periphery of each landslide. In addition, data on type of failure, failure mechanism, dimension, material involved and failed slope morphometry was also collected. In total 30 past landslides were identified in the study area (Figure 5).

These landslides have mainly failed by following four different modes; rotational, translational, fall and complex mode of failures. The translational and complex modes of failures were observed mainly in residual and alluvial soils, respectively. Further, most of the rotational mode of failure was observed in colluvial and alluvial deposits. On the other hand, rock fall in the area were observed in the disintegrated rock mass, mainly along Woldiya - Bahir Dar road section. Besides, the local administration offices were approached to collect systematic records on past landslides, particularly for landslide occurrence date, time, duration, failure mechanism etc., however no such data is being maintained by the concerned offices.
Therefore, to have such information, local residents were approached and informally interviewed through pre-designed questionnaires. According to the local respondents, most of the past landslides occurred during mid of July to September in past years. However, respondent failed to provide information on exact date and time for the past landslides in the area.

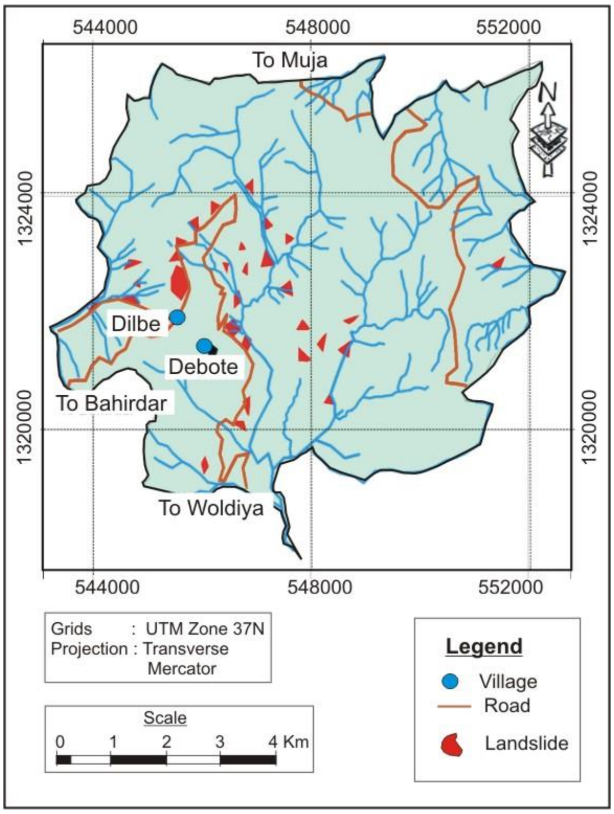

Figure 5: Landslide inventory map

Further, the meteorological data showed relatively high rainfall during this period. Thus, it can safely be concluded that main triggering factor for the past landslides in the present study area was heavy rainfall.

5.2 Causative factors evaluation

The stability of a slope is mainly governed by the causative intrinsic parameters (Raghuvanshi et al., 2014a; Wang and Niu, 2009; Ayalew et al., 2004; Anbalagan, 1992). The causative factors considered for the present study are; slope-material, slope, aspect, elevation, land use/land cover and groundwater surface traces. These causative factors were selected based on the field observations and their possible relative contribution in inducing instability to the slopes in the present study area. For the purpose of landslide hazard zonation (LHZ) in the present study, attempt was made to evaluate causative factors with respect to their quantitative relationship with the past landslides in the area.

5.2.1 Slope material

Slope material map was prepared by combining soil map and lithological map of the study area. The soil map was extracted from the soil map of Ethiopia, prepared by Food and Agriculture organization (FAOUN, 1986) whereas; lithological map was extracted from the map prepared by the Geological survey of Ethiopia (GSE, 2010). The slope material map was further verified and modified with the field survey. In the present study area, three types of soils are present, these are; residual, alluvial and collvial. The rocks exposed in the study area are classified as disintegrated and blocky rock mass (Figure 6a). In order to evaluate contribution of slope material on past landslides, overlay analysis was performed. The overlay analysis revealed that about 38.5% of past landslides has occurred in disintegrated rock mass, 27% in alluvial soils, 26% in colluvial soil and remaining 8.5% in residual soils (Figure 7).

5.2.2 Slope

The slope map of the study area was extracted from the DEM at 30m resolution from ASTER data set (Figure 6b). In general, slope inclination in the present study area varies from 0 to 70º. For the present study slope inclination was distributed into five classes; 0-5º, 5-10º, 10-25º, 25-38º and slopes >38º. These slope classes were made based on the expert decision and the general topography of the area.

The overlay analysis of the past landslides with slope inclination map revealed that 7% of the past landslides falls in 0-5º, 15% falls in 5-10%, 27% falls in 10-25º, 20% falls in 25-38º and 31% falls in the slope class >38º (Figure 7). About 51% of the past landslides fall in slopes having inclination greater than 25º. Also, about 42% of the past landslides were observed in the gentle slope sections (slope inclination 5 – 25º). It was observed that slopes having inclination in between 5 – 25º are mostly occupied by unconsolidated material which is considered to be highly susceptible for the slope instability (Raghuvanshi et al., 2014a: 2014b).

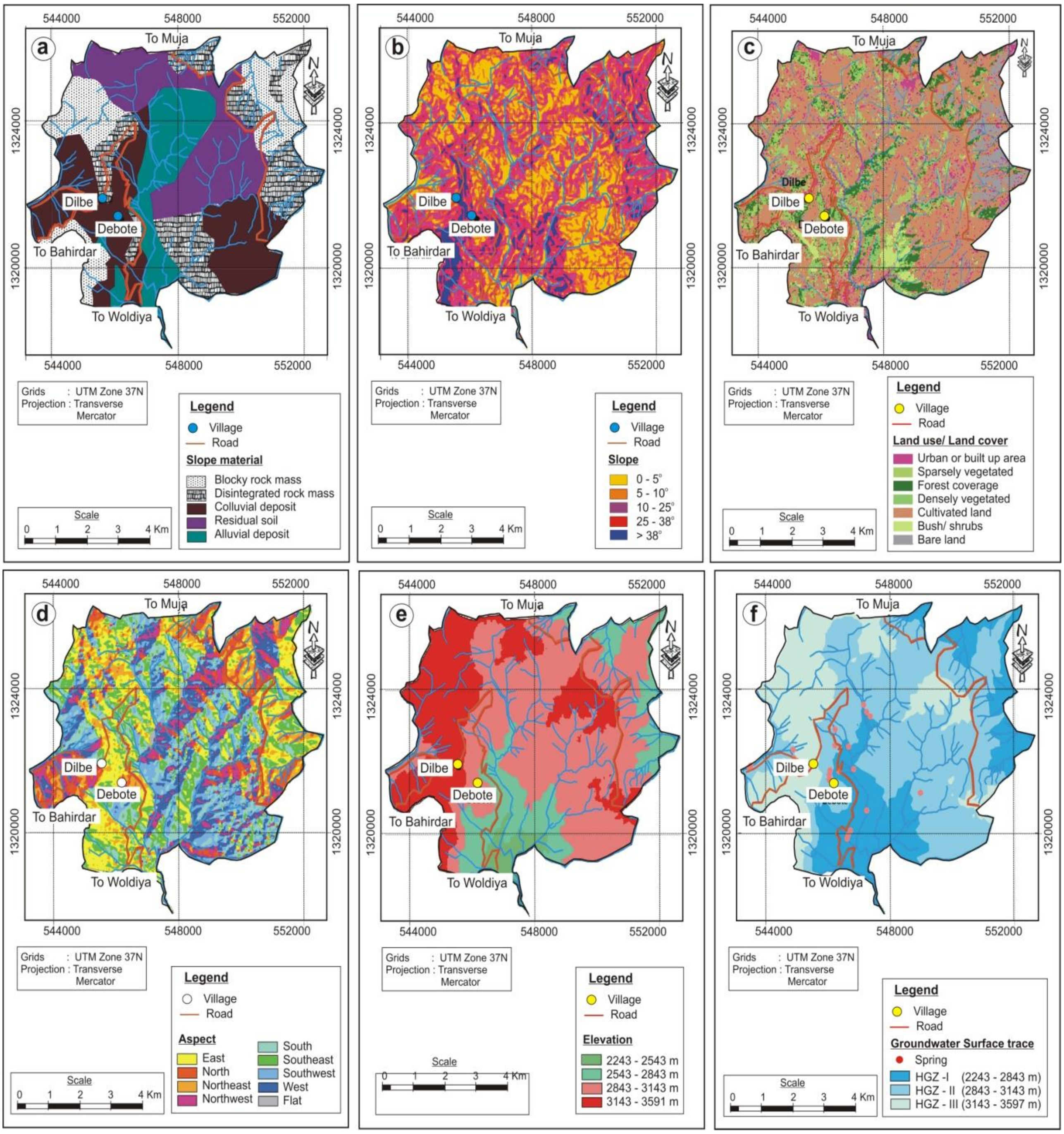

Figure 6: Causative factors map - (a) slope material, (b) slope, (c) land use and land cover, (d) aspect, (e) elevation and (f) ground water surface trace

5.2.3 Aspect

For the present study the aspect map was extracted from the DEM at 30m resolution from ASTER data set. For the present study aspect has been classified as; (i) Flat (1), (ii) North (0– 22.5º), (iii) North-east (22.5–67.5º), (iv) East (67.5–112.5º), (v) South-east (112.5–157.5º), (vi) South (157.5–202.5º), (vii) South-west (202.5–247.5º), (viii) West (247.5–292.5º), (ix) North-west (292.5–337.5º), and (x) North (337.5-365^0) (Figure 6d). The overlay analysis revealed that 20%, 18% and 16% of the past landslides occurred in the slopes that are inclined towards South, Southeast and East directions, respectively. Further, 11.2%, 9.2% and 7.7% of landslides occurred on slopes that are oriented towards Southwest, North and Northeast directions, respectively (Figure 7). On the other hand, slopes oriented towards West and Northwest directions have 7.68% and 6.62% of landslides, respectively

5.2.4 Elevation

The elevation of the study area was extracted from the DEM at 30m resolution from ASTER data set. The elevation of the study area was classified into four classes; 3143-3597m, 2843-3143m, 2543-2843m and 2243-2543m (Figure 6e). The overlay analysis showed that about 35% of the past landslides occurred in elevation class of 2243-2543m, 31.5% occurred in 2543-2843m elevation class, 26% occurred in elevation class 2843-3143m and the remaining 7.5% landslides occurred in elevation class 3143-3597m (Figure 7). From these results it can be noticed that about 66.5% past landslides occurred in two elevation classes, 2243-2543m and 2543-2843m.

5.2.5 Land use and Land cover

For the present study land use and land cover map was prepared from the Sentinel-2A data through supervised classification by using ERDAS Imagine. The land use and land cover of the present study area was classified into seven classes; urban or built up area, bare land, bush or shrubs land, sparsely vegetated land, densely vegetated area, forest coverage and cultivated land (Figure 6c). The overlay analysis showed that 26.3% of past landslides fall in the sparsely vegetated land, 24% of landslide falls in Bush or shrubs land, 20% of landslide falls in cultivated land, 8.4% falls in forest coverage, 7.7% falls in densely vegetated area, 7% falls in built up area and remaining 6.6% landslides falls in bare land (Figure 7). The results show that about 70% of the past landslides are concentrated in three classes; sparsely vegetated land, bush or shrubs land and cultivated land. As observed, these land use and land cover classes are mainly occupied by disintegrated rock mass, colluvial and alluvial soils. These unconsolidated materials are susceptible for slope instability (Raghuvanshi et al., 2014b).

5.2.6 Ground water condition

Groundwater is the most important factor that is responsible in inducing instability to the slopes (Raghuvanshi et al., 2014a; Girma et al., 2015; Chimidi et al., 2017). Assessment of groundwater condition throughout the area is practically not feasible for landslide hazard evaluation studies. However, groundwater condition can be assessed by indirect means of surface manifestations, such as presence of springs over the slopes (Anbalagan, 1992; Chimidi et al., 2017).

Presence of springs on the slope face is an indication of proximity to groundwater and it also suggests general saturation of the slope material. It is also believed that spring locations have direct correlation with the landslides occurrences (Girma et al. 2015; Raghuvanshi et al., 2015; Chimidi et al., 2017). In the present study 22 springs were identified in the field during the inventory mapping. Thus, with the help of spring density and the respective elevation range, hydrological homogeneous zones were delineated in the study area (Raghuvanshi et al., 2015).

The hydrological homogeneous zones that were delineated in the study area are; HGZ-I (2243-2843m), HGZ-II (2843-3143m) and HGZ-III (3143-3597m) (Figure 6f). The overlay analysis with the past landslide data clearly indicates that 46.8% landslides fall in HGZ-I (2243-.2843m) zone, 33.2% falls in HGZ-II (2843-3143m) zone and the remaining 20% landslides fall in HGZ-III (3143-3597m) zone (Figure 7).

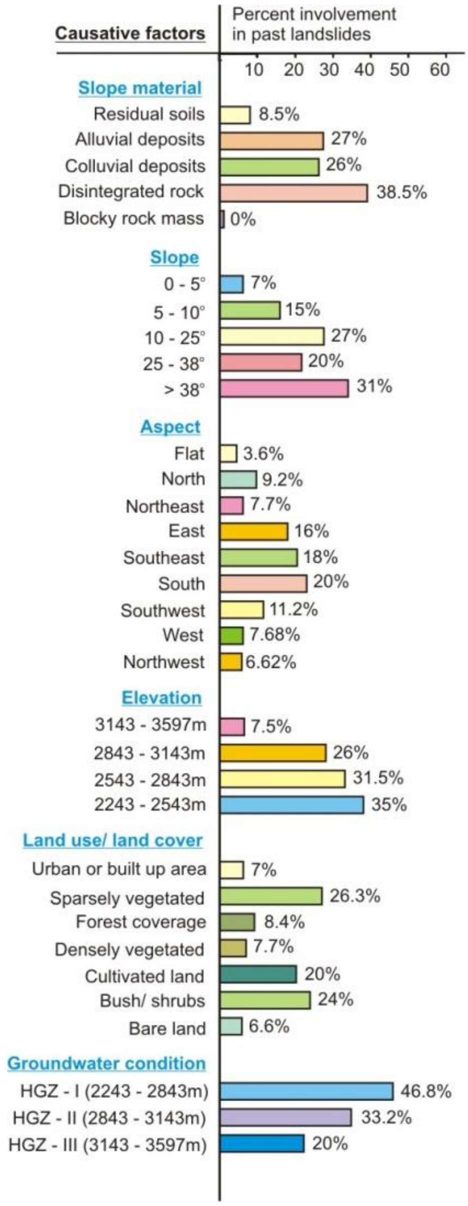

Figure 7: Causative factors influence on past landslide

5.3 Landslide Susceptibility Index (LSI)

Through landslide inventory data it is possible to understand the relative contribution of various causative factors on landslides in the area. The general assumption in this regard is that "the past and the present is the key for the future". It means that the conditions that were responsible to initiate landslides in the past if reoccur in some other area; again landslides can occur (Dai et al., 2002; Lan et al., 2004; Chimidi et al., 2017). Thus, to understand the quantitative relationship between the past landslides and the factor sub-class of each causative factor Landslide Susceptibility Index (LSI) was computed. The LSI was originally proposed by Sarkar et al., (1995) and later it was modified by Raghuvanshi et al., (2015) and is expressed by Eq.1

$$LSI = Hazardindex * \frac{LSV}{100} \qquad \ldots.. (1)$$

Where; 'LSI' is the Landslide Susceptibility Index, 'LSV' is the Landslide susceptibility value and 'Hazard index' is the ratio between ''total pixel counts of a sub-class within a Landslide" to the ''total pixel count of that sub-class in the area of study".

In order to calculate LSI for each sub-class of the causative factors, raster calculator tool in ArcGIS was used and Hazard index for each sub class of causative factors was determined.By overlaying the past landslide map over each factor map, total pixel count of a sub-class within area covered by Landslide and the total pixel count of that sub-class in the area of study were determined. Through the raster calculator in ArcGIS, it was found that the total number of pixels for the entire study area is 54257 whereas the number of pixels covered by the landslide is equal to 1020. Table 2 shows the total pixel counts of a sub-class of each causative factor within a Landslide and the total pixel count of that sub-class in the area of study. Further, based on the comparative significance of each causative factor in inducing landslides in the area, LSV were assigned to each causative factor. These LSVs were assigned on a scale of 100 with proportionate distribution to respective causative factors. Landslide is a complex process and it is resulted from contributions of various causative factors. Practically, it is not possible to evaluate contributions of each causative factor in quantitative terms however, through expert evaluation an effort was made to assign LSV to respective causative factors based on the observations made on the past landslide activities in the study area and through the evaluation of the terrain condition (Raghuvanshi et al., 2015). LSV values thus, assigned to the respective causative factors are presented in Table 2. Through past landslide inventory data it was realized that slope material, groundwater surface trace and land use and land cover factors are relatively most prominent factors and have almost contributed significantly for landslide occurrence in the study area. Thus, a LSV value of 20 was assigned to each of these causative factors. Further, elevation and slope factors were found to be less significant therefore these factors were assigned with a LSV value of 15 each. Aspect was given a LSV value of 10, as it was not found to be relatively significant.

5.4: Grid overlay analysis for landslide hazard evaluation

In order to perform geo-processing by overlay analysis the entire study area was divided into 10 x 10m regular square polygon cells. For this a grid was prepared in AutoCAD map where the study area boundary was imported and a grid with 10 x 10m was created. The total study area (50 sq km) was covered by 5226 polygon grid cells. Later, this grid file was exported as a shape file. In order to assign unique IDs to each grid cell '*.dbf' component of the shape file was edited in MS Excel program and unique IDs to each grid cells (1 to 5226) were assigned. Later, this grid file was utilized for overlay analysis with each causative factor maps in GIS environment. Further, the grid file was overlaid on each individual causative factor themes and geo-processing was done.

The primary purpose of this geo-processing was to know the presence of various factor sub-classes in each grid cell. Thus, the overlay analysis resulted into six files, each containing grid cells with various sub-classes of respective causative factors. Later, all six geo-processed causative factor themes were merged together by using 'merge theme' option in ArcMap. Finally, a single composite grid file showing intersection with various sub-classes of all six causative factors were obtained. This composite geo-processed grid file also showed attribute data for specific factor sub-classes in 6 columns for each grid cells. Later, '*.dbf' component of composite grid shape file was edited in MS Excel and corresponding LSI values were assigned to each factor sub-class by using find and replace command in MS Excel. Further, for each grid cell LSI values for all 6 causative factors were summed up to get a Total Landslide Susceptibility value (TLSI). Finally, these TLSI values, obtained for each grid cell, formed the basis for the Landslide Hazard Zonation (LHZ) of the study area.

5.5 Landslide Hazard Zonation (LHZ)

For the present study area the minimum TLSI value was found to be 0.58 and the maximum value was 1.34. Further, the TLSI values were classified into various hazard classes as; very low hazard (VLH), low hazard (LH), moderate hazard (MH), high hazard (HH) and very high hazard (VHH). The initial distribution of the TLSI values for various hazard classes was based on logical judgment. Later, attempts were made on trial basis by considering different distributions of TLSI values for various hazard classes and the corresponding LHZ maps were prepared. For every such attempts overlay analysis was made to validate the LHZ map with the past landslide inventory map. Thus, the TLSI values for various hazard classes that gave the best validation with the past landslide data was finally considered. The TLSI values distributed for various landslide hazard classes used to prepare the final LHZ map for the present study is presented in Table 3. Further, the LHZ map prepared during the present study is presented as figure 8. A perusal of figure 8 clearly shows that 11.55% (5.78km^2) of the study area falls into 'very high hazard' (VHH), 19.84% (9.92km^2) area falls into 'high hazard' (HH), 14.36% (7.18km^2) area falls into 'medium hazard' (MH), 38.25% (19.13km^2) area falls into 'low hazard' (LH) and remaining 16% (8km^2) of area falls into 'very low hazard' (VLH).

Table 2: Landslide causative factor classes with their respective LSV and LSI

Causative factors and corresponding factor class	Pixel count for Landslide did not occur		Pixel count for Landslide occurred		Hazard index	Landslide Susceptibility Index	Landslide Susceptibility Value
	Count	Ratio (a) ~~%~~	Count	Ratio (b) ~~%~~	(b/a)	LSI	LSV
(a) Slope materials							
Residual soils	12043	22.20	58	5.69	0.26	0.052	
Alluvial deposits	8141	15.00	261	25.59	1.71	0.342	
Colluvial deposits	15053	27.74	272	26.67	0.96	0.192	20
Disintegrated rock mass	10705	19.73	429	42.06	2.13	0.426	
Blocky rock mass	8315	15.33	0	0.00	0.00	0.000	
Total	54257	100.00	1020	100.00			
(b) Slope							
0-5	12076	22.26	175	17.16	0.77	0.116	
5-10	16498	30.41	270	26.47	0.87	0.131	
10-25	13452	24.79	299	29.31	1.18	0.177	15
25-38	8914	16.43	189	18.53	1.13	0.170	
>38	3317	6.11	87	8.53	1.40	0.210	
Total	54257	100.00	1020	100.00			
(c) Aspect							
Flat (0°)	375	0.69	16	1.57	2.28	0.227	
N (0°-22.5°)	2496	4.60	18	1.76	0.38	0.038	
NE (22.5°-67.5°)	6147	11.33	107	10.49	0.93	0.093	
E (67.5°-112.5°)	9374	17.28	220	21.57	1.25	0.125	
SE (112.5°-157.5°)	8122	14.97	192	18.82	1.26	0.126	
S (157.5°-202.5°)	6701	12.35	143	14.02	1.14	0.114	10
SW (202.5°-247.5°)	6728	12.40	117	11.47	0.93	0.093	
W (247.5°-292.5°)	6393	11.78	104	10.20	0.87	0.087	
NW (292.5°-337.5°)	5678	10.47	83	8.14	0.78	0.078	
N (337.5°-360°)	2243	4.13	20	1.96	0.47	0.047	
Total	54257	100.00	1020	100.00			
(d) Elevation							
2243-2543	6319	11.64	185	18.14	1.56	0.234	
2543-2843	14191	26.16	361	35.39	1.35	0.203	
2843-3143	24401	44.97	276	27.06	0.60	0.090	15
3143-3597	9346	17.23	198	19.41	1.13	0.170	
Total	54257	100.00	1020	100.00			
(e) Land-use and Land-cover							
Urban/ built up area	3593	6.63	60	5.88	0.89	0.178	
Forest coverage	4580	8.44	80	7.84	0.93	0.186	
Densely vegetated	3371	6.21	60	5.88	0.95	0.190	
Cultivated land	31290	57.67	566	55.5	0.96	0.194	20
Bare Land	4368	8.05	87	8.53	1.06	0.212	
Sparsely Vegetated	5757	10.61	137	13.43	1.27	0.254	
Bush land	1298	2.39	30	2.94	1.23	0.246	
Total	54257	100.00	1020	100.00			
(f) Ground water surface traces							
HGZ-I (2243-2843)	12600	23.22	300	29.41	1.27	0.254	
HGZ-II (2843-3143)	28321	52.20	520	50.98	0.98	0.196	20
HGZ-III (3143-3597)	13336	24.58	200	19.61	0.80	0.160	
Total	54257	100.00	1020	100.00			

6. Results and discussion

6.1 Causative factors relation with landslides

The landslide inventory carried out during the present study showed the presence of 30 past landslides in the study area. These landslides are mainly present in the central, western and the southern parts of the study area (Figure 5). The landslides, as observed in the study area, have failed by following fall, transitional, rotational and complex mode of failures. Out of total observed landslides 76% has failed by rotational mode of failure, 17% failed as fall and remaining 7% as translational and complex mode of failures. Most of the rotational mode of failure was observed in colluvial and alluvial deposits whereas transitional and complex modes of failures were observed mainly in the residual and alluvial soils, respectively. Besides, rock fall in the area were mainly observed in disintegrated rock mass. As revealed by the local respondents all these landslides in the present study area have occurred during the rainy season (mid of July-September). This indicates that the main triggering factor for past landslides in the study area is heavy rainfall.

Table 3; Landslide hazard zonation based on Total Landslide Susceptibility Index (TLSI) value

No	Value for zonation	Zone Designation	Class
1	0.58-0.78	VLH	Very low hazard
2	0.79-0.99	LH	Low hazard
3	1.00-1.11	MH	Moderately hazard
4	1.12-1.33	HH	High hazard
5	>1.33	VHH	Very high hazard

Further, past landslide data revealed that about 38.5% landslides occurred in disintegrated rock mass, 27% in alluvial soils, 26% in colluvial soil and the remaining 8.5% in residual soils. No landslides were recorded in the blocky rock mass. These figures clearly show that 61.5% of landslides have occurred in slopes that are covered by alluvial, colluvial or residual soils and 38.5% of landslides occurred in disintegrated rock mass. The analysis further revealed that probability of landslides is high in disintegrated rock mass and the alluvial deposits as the Hazard index values are 2.13 and 1.71, respectively (Table 2). It may be noted that, Hazard index value of greater than ‘1’ indicates more probability of the landslide occurrence (Girma et al. 2015; Chimidi et al. 2017). Perusal of Table 2 shows that slope material classes; residual soils and blocky rock mass have relatively less probability for landslide occurrence as the hazard index values for these classes is less than ‘1’. Also, colluvial material shows hazard index value equal to 0.96 which is nearly close to 1; thus indicating some probability for landslide occurrence. High concentration of landslides in the slopes covered by the unconsolidated materials; disintegrated rock mass, alluvial deposits and colluvial deposits is related to the low shear strength of the material. Also, such material when saturated may become more prone for instability (Anbalagan 1992; Raghuvanshi et al. 2014a; 2014b).

The overlay analysis of past landslides with slope inclination map further revealed that 31% of landslides fall in slope class > 38°, 27% fall in slope class 10-25° and 20% in slope class 25-38°. Also, it was found that the hazard index values for slope classes; >38°, 10-25° and 25-38° are 1.4, 1.18 and 1.13, respectively (Table 2). Since all these hazard index values are greater than ‘1’ therefore it shows that the slope classes >38°, 10-25° and 25-38° are more susceptible for landslides. The high concentration of landslides in steeper slope sections are possibly related to the fact that as the slope becomes steeper the shear stress and tangential component of weight within the slope increases, thus tendency of slope instability increases (Ahmed 2009; Raghuvanshi et al. 2015). Also, about 42% of the past landslides were observed in the gentle slope sections (slope inclination 5 – 25°). It was observed that slopes having inclination in between 5 – 25° in the study area are mostly occupied by unconsolidated material which is considered to be highly susceptible for the slope instability (Raghuvanshi et al. 2014a: 2014b).

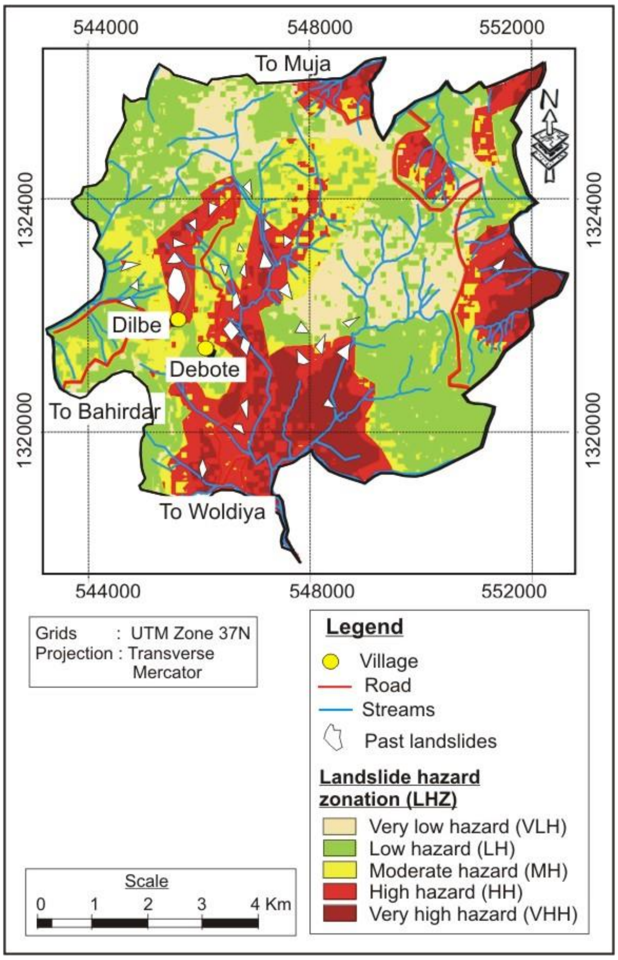

Figure 8: Landslide Hazard Zonation (LHZ) map

The overlay analysis of past landslides with aspect map showed that about 54% of the past landslides occurred on the slopes that are oriented towards South, Southeast and East directions. Also, it was found that hazard index values for aspect classes South, Southeast and East are 1.14, 1.26 and 1.25, respectively. Since all these hazard index values are greater than ‘1’, therefore slope sections which are inclined towards South, Southeast and East directions show more probability for landslide occurrence. Further, when past landslides are compared to the distribution of springs in the area, it was found that most of the springs are present on the slopes that are inclined towards South or East directions. Thus, the high concentration of the past landslides in the area may possibly be related to the general groundwater flow direction, presence of unconsolidated material over the slopes and oversaturated slope material. All these conditions are responsible for slope instability which might have possibly resulted into landslides (Arora 1997; Hoek and Bray 1981; Raghuvanshi et al. 2014a).

The overlay analysis between past landslides and the elevation map of the study area showed that about 66.5% past landslides occurred in two elevation classes, 2243-2543m and 2543-2843m. Also, the hazard index values computed for the elevation classes 2243-2543m and 2543-2843m are 1.56 and 1.35, respectively (Table 2). These hazard index values clearly show that elevation classes 2243-2543m and 2543-2843m are susceptible for slope instability as these hazard index values are greater than '1'. Further, it was observed that these elevation classes in the study area are dominated by high concentration of springs, disintegrated rock mass, colluvial and alluvial soils. Besides, slopes on theses elevation classes are being utilized for cultivation purpose. Cultivation practice may possibly trigger slope instability by frequent unplanned irrigation that saturates unconsolidated material (Raghuvanshi et al. 2014a). Further, disintegrated rock mass, colluvial and alluvial soils with presence of springs make these slopes more susceptible for instability (Raghuvanshi et al. 2015).

The past landslide data also showed that 26.3% of past landslides fall in the sparsely vegetated land, 24% of landslide falls in Bush land and 6.6% of landslides fall in bare land. Also, Hazard index values for sparsely vegetated land, bush land and bare land are 1.27, 1.23 and 1.06, respectively (Table 2). Since, hazard index values for sparsely vegetated land, bush land and bare land are greater than '1' therefore these land use and land cover classes have more probability for landslide occurrence. Further, it was also observed that these land use and land cover classes are mainly occupied by disintegrated rock mass, colluvial and alluvial soils. These unconsolidated materials are susceptible for slope instability (Raghuvanshi et al. 2014b).

The past landslides data further showed that about 80% of the landslides fall within hydrological homogeneous zone classes HGZ-I and HGZ-II. Also, Hazard index value for HGZ-I class is 1.27 which shows high probability for landslide occurrence (Table 2). Similarly, Hazard index value for HGZ-II class is 0.98 which is nearly close to '1' thus it also shows relative probability for landslide occurrence. The high concentration of landslides in HGZ-I and HGZ-II zones show direct relation of landslides with the springs in the area. Also, it may be seen that HGZ-I and HGZ-II zones are dominated by disintegrated rock mass, colluvial and alluvial soils. These materials have weak shear strength and become more susceptible to instability when they are relatively saturated (Raghuvanshi et al. 2015). Thus, all these conditions make HGZ-I and HGZ-II zones more susceptible for slope instability. For this reason, only about 80% of the landslides fall within hydrological homogeneous zones HGZ-I and HGZ-II in the study area.

6.2 Landslide hazard zonation (LHZ) - distribution

Landslide hazard evaluation shows that 11.55% (5.78km^2) of the study area falls into 'very high hazard' (VHH), 19.84% (9.92km^2) area falls into 'high hazard' (HH), 14.36% (7.18km^2) area falls into 'medium hazard' (MH), 38.25% (19.13km^2) area falls into 'low hazard' (LH) and remaining 16% (8km^2) of area falls into 'very low hazard' (VLH). Further, perusal of Fig. 8 shows that VHH and HH zones are mainly concentrated in the southern, northern and eastern parts of the study area. The area delineated as VHH and HH zones have good concentration of springs. In general, it has been observed that spring locations generally have direct correlation with the landslides occurrences (Girma et al. 2015; Raghuvanshi et al. 2015; Chimidi et al. 2017). Also, majority of the areas in VHH and HH zones have slopes that are inclined at 10 to 38^o and generally have unconsolidated deposits and disintegrated rock mass. As stated earlier, the unconsolidated materials and disintegrated rock mass have relatively low shear strength and such material when saturated may become more prone for instability (Anbalagan 1992; Raghuvanshi et al. 2014a; 2014b). Further, the MH zones are distributed towards Northern, Central and Western regions of the study area (Figure 8). On the other hand; LH zones are scattered in the study area. The VLH zones are mainly concentrated in the Northern and the Eastern parts of the study area. Also, VLH and LH zones fall mainly in slopes that are inclined at slope angles less than 5^o and are mainly composed of blocky rock mass.

6.3 LHZ map validation

In order to check the validity of the LHZ map, prepared during the present study, an overlay analysis was made with the past landslides activity in the area (Figure 8). It is believed that if the past landslides fall either within high hazard (HH) or very high hazard (VHH) zones the prepared LHZ map is validated and it has possibly delineated all hazard zones appropriately in the study area. The overlay analysis results showed that 74% (22) of the past landslides fall within VHH and HH zones of the prepared LHZ map. Further, 17% (5) of the past landslides fall into moderate hazard (MH) zone that also have reasonable probability of landslide occurrence. Only 9% (3) of the past landslides fall within low hazard (LH) and very low hazard (VLH) of the LHZ map. Thus, it may be concluded from these results that the prepared LHZ has reasonably validated with the past landslide data. About 9% of the past landslides that fall within LH or VLH zones do not validate with the prepared LHZ map. This variation in the validity of the LHZ map may be due to the limitation of the methodology followed in the present study. The present study was conducted on medium scale and many factors that are responsible for instability of slopes cannot be considered at this scale (Ayele et al. 2014). These factors are discontinuity characteristics and the relationship of discontinuities with the slope, water pressures within the slope, shear strength of the material along the potential discontinuity surfaces etc. (Girma et al. 2015; Chimidi et al. 2017; Hamza and Raghuvanshi 2017).

7. Conclusion

Landslide hazard evaluation in the present study shows that 11.55% (5.78km^2) of the study area falls into 'very high hazard' (VHH), 19.84% (9.92km^2) area falls into 'high hazard' (HH), 14.36% (7.18km^2) area falls into 'medium hazard' (MH), 38.25% (19.13km^2) area falls into 'low hazard' (LH) and remaining 16% (8km^2) of area falls into 'very low hazard' (VLH). Further, validation results showed that 74% (22) of the past landslides fall within VHH and HH zones of the prepared LHZ map. Further, 17% (5) of the past landslides fall into moderate hazard (MH) zone that also have reasonable probability of landslide occurrence. Only 9% (3) of the past landslides fall within low hazard (LH) and very low hazard (VLH) of the LHZ map. The prepared LHZ map has reasonably validated with the past landslide data. Finally, in general it may be concluded that about 31% area falls into VHH and HH zones and about 14% of the area falls into MH zone. Thus, about 45% of the area is prone for the landslide hazard. The major factors responsible for landslide hazard in the area are the susceptible slope material comprising mainly; disin-tegrated rock mass, alluvial, colluvial and residual soils. Also, slopes that are inclined at moderate to steep slope angles and are oriented towards South, Southeast and East directions are more susceptible for instability. Besides, slopes which fall in between elevations 2243 to 2843m have also shown potential instability. The landslides in the study area have been triggered mainly during the rainy season. Since the landslides in the area have been causing considerable damage to the roads, houses and the agricultural land therefore there is a need to implement mitigation measures, particularly in hazardous zones delineated through the present study.

Acknowledgements

We thankfully acknowledge all kinds of support extended to us by the head and the staff of the School of Earth Sciences, College of Natural and Computational Sciences, Addis Ababa University. The meticulous review and comments by the esteemed anonymous reviewers is also duly acknowledged.

References

Abebe, B., F. Dramis, G. Fubelli, M. Umer and A. Asrat (2010). Landslides in the Ethiopian highlands and the rift margins, Journal of African Earth Sciences, 56, 131–138.

Ahmed, S. (2009). Slope stability analysis using GIS and numerical modeling techniques (Unpublished MSc thesis), Vrije Universiteit, Brussel.

Anbalagan, R. (1992). Landslide hazard evaluation and zonation mapping in mountainous terrain, Engineering Geology, 32, 269–277.

Arora, K.R. (1997). Soil mechanics and foundation engineering, Standard Publishers Distributers, Delhi, India, pp. 475.

Arnous, M.O. (2011). Integrated remote sensing and GIS techniques for landslide hazard zonation: a case study WadiWatier area, South Sinai, Egyptian Journal of Coastal Conservation15, 477-497

Ayalew, L., H. Yamagishi and N. Ugawa (2004). Landslide susceptibility mapping using GIS-based weighted linear combination, the case in Tsugawa area of Agano River, Niigata Prefecture, Japan, Landslides, 1, 73–81.

Ayalew, L. and H. Yamagishi (2004). Slope failures in the Blue Nile basin, as seen from landscape evolution perspective, Geomorphology, 61, 1–22.

Ayele, S., T.K. Raghuvanshi and P.M. Kala (2014). Application of remote sensing and GIS for landslide disaster management—a case from Abay Gorge, Gohatsion–Dejen section, Ethiopia. Landscape ecology and water management, proceedings of International Geographical Union (IGU) Rohtak Conference, Advances in Geographical and Environmental Sciences (M. Singh, R.B. Singh and M.I. Hassan: Editors),. Springer, Japan, Vol. 2, pp. 15–32

Ayenew, T. and G. Barbieri (2005). Inventory of landslides and susceptibility mapping in the Dessie area, Northern Ethiopia, Engineering Geology, 77, 1–15

Bommer, J. J. and C. E. Rodrı'guez (2002). Earthquake-induced landslides in Central America. Engineering Geology, 63,189–220

Carrara, A., M. Cardinali and F. Guzzetti (1992). Uncertainty in assessing landslide hazard and risk, ITC Journal, 2, 172–183

Carrara, A., M. Cardinali, R. Detti, F. Guzzetti, V. Pasqui and P. Reichenbach (1991). GIS techniques and statistical models in evaluating landslide hazard. Earth Surface Process Landform, 6, 427–445

Casagli, N., F. Catani, C. Puglisi, G. Delmonaco, L. Ermini and C. Margottini (2004). An inventory-based approach to landslide susceptibility assessment and its application to the Virginio River Basin. Italy Environ, Journal of Environmental and Engineering Geosciences, 10 (3), 203–216

Chimidi, G., T. K., Raghuvanshi and K. V. Suryabhagavan (2017). Landslide hazard evaluation and zonation in and around Gimbi town, western Ethiopia – a GIS-based statistical approach, Journal of Applied Geomatics, 9 (4), 219–236.

Collison A., S. Wade, J. Griffiths and M. Dehn (2000). Modelling the impact of predicted climate change on landslide frequency and magnitude in SE England, Engineering Geology, 55, 205–218

Crozier, M.J. and T.Glade (2005). Landslide hazard and risk: issues, concepts, and approach. Glade, Landslide

Hazard and Risk, (T. Anderson and M. Crozie: Editors) Wiley, Chichester, pp. 1–40

Dahal, R.K., S.Hasegawa, T.Masuda and M.Yamanaka (2006). Roadside slope failures in Nepal during torrential rainfall and their mitigation. Disaster Mitigation of Debris Flows, Slope Failures and Landslides, pp 503–514

Dai, F. C., C. F. Lee and Y. Y. Ngai (2002). Landslide risk assessment and management: an overview. Engineering Geology, 64, 65–87

Dai, F. C. and C. F. Lee (2001). Terrain-based mapping of landslide susceptibility using a geographical information system: a case study, Canadian Geotechnical Journal, 38, 911–923

Demissie, T., G. Yohannes, A. Mammo, Y. Tesfaye, Y. Teshome, G. Burusa, M. Edris and M. Wenduante (2010). Geology geochemistry and gravity survey of the Dessie area, unpublished report, pp. 68.

Ermias, B., T. K. Raghuvanshi and B. Abebe (2017). Landslide Hazard Zonation (LHZ) around Alemketema Town, North Showa Zone, Central Ethiopia - A GIS based expert evaluation approach International Journal of Earth Sciences and Engineering, 10 (1), 33 -44

Fall, M., R. Azzam and C. Noubactep (2006). Amulti-method approach to study the stability of natural slopes and landslide susceptibility mapping, Engineering Geology, 82, 241–263

FAOUN (Food and Agriculture Organization of the United Nations) (1986). Ethiopian highlands reclamation study, Food and Agriculture Organization of the United Nations, Rome, pp. 334

Gemechu, D. (1977). Aspect of climate and water balance in Ethiopia. Addis Ababa University press, Addis Ababa, pp. 79

Girma, F., T.K. Raghuvanshi, T. Ayenew and T. Hailemariam (2015). Landslide hazard zonation in AddaBerga District, Central Ethiopia—a GIS based statistical approach, Journal of Geomatics, 9, 25–38

Gorsevski, P.V., P. Jankowski and P.E. Gessler (2006). A heuristic approach for mapping landslide hazard by integrating fuzzy logic with analytic hierarchy process. Control Cybernet, 35 (1), 121–146

GSE (Geological Survey of Ethiopian), (2010). Geosciences Report on Dessie area, Unpublished Report, Geological Survey of Ethiopian, Addis Ababa, Ethiopia, pp. 68

Guzzetti, F., A. Carrara, M. Cardinali and P. Reichenbach (1999). Landslide hazard evaluation: a review of current techniques and their application in a multi-scale study, central Italy. Geomorphology, 31(1–4), 181–216

Hamza, T. and T. K. Raghuvanshi (2017). GIS based landslide hazard evaluation and zonation—a case from Jeldu District, Central Ethiopia. Journal of King Saud University–Science, 29, 151–165

Hoek, E and J. W. Bray (1981). Rock slope engineering (revised third edition). Institute of Mining and Metallurgy, London, pp. 358

Kanungo, D. P., M. K. Arora, S. Sarkar and R.P. Gupta (2006). A comparative study of conventional, ANN black box, fuzzy and combined neural and fuzzy weighting procedures for landslide susceptibility zonation in Darjeeling Himalayas, Engineering Geology, 85,347–366

Keefer, D. V. (2000). Statistical analysis of an earthquake-induced landslide distribution—the 1989 Loma Prieta, California event. Engineering Geology, 58, 231–249

Lan, H. X., C. H. Zhou, L. J. Wang, H. Y. Zhang and R. H. Li (2004). Landslide hazard spatial analysis and prediction usingGIS in the Xiaojiang watershed, Yunnan. China, Engineering Geology, 76, 109–128

Lee, S., J.H. Rhyu, J. S. Won and H. J. Park (2004). Determination and application of the weights for landslide susceptibility mapping using an artificial neural network at south. Korean Engineering Geology, 71, 289–302

Leroi, E. (1997). Landslide risk mapping: problems, limitation and developments. Landslide risk assessment, (F. Cruden : Editor), Balkema, Rotterdam, pp. 239–250

Marrapu, B. M and R. S. Jakka (2014). Landslide Hazard Zonation Methods: A Critical Review, International Journal of Civil Engineering Research, 5, 215-220

Pan, X., H. Nakamura, T. Nozaki and X. Huang (2008). A GIS-based landslide hazard assessment by multivariate analysis Landslides. Journal of Japan Landslide Society, 45 (3), 187–195.

Parise, M. and R.W. Jibson (2000). A seismic landslide susceptibility rating of geologic units based on analysis of characteristics of landslides triggered by the 17 January, 1994 Northridge, California earthquake, Engineering Geology, 58, 251–270

Raghuvanshi, T. K., L. Negassa and P.M. Kala (2015). GIS based grid overlay method versus modeling approach—a comparative study for landslide hazard zonation (LHZ) in Meta Robi District of west Shewa Zone in Ethiopia. Egyptian Journal of Remote sensing and Space Science, 18(2), 235–250

Raghuvanshi, T. K., J. Ibrahim and D. Ayalew (2014a). Slope stability susceptibility evaluation parameter (SSEP) rating scheme—an approach for landslide hazard zonation. Journal of African Earth Sciences, 99, 595–612

Raghuvanshi, T.K., P.M. Kala and M. Singh (2014b). Landslide disaster management and reduction- An approach through remote rensing and GIS. Landscape ecology and water management, proceedings of International Geographical Union (IGU) Rohtak Conference, Advances in Geographical and Environmental Sciences (M. Singh, R.B. Singh and M.I. Hassan: Editors), Springer, Japan, Vol. 2, Springer Japan, pp. 33-40

Sarkar, S. and D.P. Kanungo (2004). An integrated approach for landslide susceptibility mapping using remote sensing and GIS, Photogrammetric Engineering & Remote Sensing, 70 (5), 617–625

Sarkar, S., D.P. Kanungo and G.S. Mehrotra (1995). Landslide hazard zonation: a case study in Garhwal Himalaya, India, Mountain Research and Development, 15 (4), 301–309.

Tefera, M., T. Chernet and W. Haro (1996). Explanation of the geological map of Ethiopia, Ethiopian Institute of Geological Surveys, Addis Ababa, 3: 79

Van Den Eeckhaut M., P. Reichenbach, F. Guzzetti, M. Rossi and J. Poesen (2009). Combined landslide inventory and susceptibility assessment based on different mapping units: An example from the Flemish Ardennes, Belgium. Journal of Natural Hazards Earth System Science, 9, 507–521.

Varnes, D.J. (1996). Landslide Types and Processes, Landslides: investigation and mitigation, transportation Research Board Special Report 247, (A.K. Turner and R.L Schuster: Editors), National Academy Press, National Research Council, Washington, D.C, pp. 36-75

Varnes, D.J. (1984). Landslide hazard zonation: a review of principles and practice. UNESCO, Paris, pp. 1–63

Wang, X. and R. Niu (2009). Spatial forecast of landslides in three gorges based on spatial data mining, Sensors, 9, 2035–2061

WestenVan, C. J., N. Rengers and M. T. J. Terlien (1997). Prediction of the occurrence of slope instability phenomena through GIS-based hazard zonation. Geologische Rundschau, 86, 4004–441